Molecular Physics, 1998, Vol. 94, No. 1, 105–119

# Explicitly correlated coupled cluster calculations of the dissociation energies and barriers to concerted hydrogen exchange of $(HF)_n$ oligomers ($n = 2, 3, 4, 5$)

By WIM KLOPPER[†][‡], MARTIN QUACK[‡] and MARTIN A. SUHM[‡][§]
[†] Department of Chemistry, University of Oslo, PO Box 1033 Blindern, N-0315 Oslo, Norway
[‡] Laboratorium für Physikalische Chemie der ETH Zürich (Zentrum), CH-8092 Zürich, Switzerland

The electronic dissociation energies and barriers to concerted hydrogen exchange of $(HF)_n$ oligomers with $n = 2, \ldots, 5$ are computed by means of a many-body decomposition of the total electronic energy. The one- and two-body terms are obtained from explicitly correlated coupled cluster calculations including singles, doubles, and a perturbative triples correction (CCSD(T)-R12), in a large Gaussian basis set consisting of 276 contracted atomic functions. The three-body term is computed at the conventional CCSD(T) level in a basis set containing 228 functions. The four- and five-body terms are obtained from explicitly correlated second-order perturbation theory calculations (MP2-R12), using basis sets with 305 (tetramer) and 380 (pentamer) functions. Since the many-body terms are computed using the same basis set (i.e. the basis of the largest fragment) for all fragments and subfragments, our calculations implicitly include a counterpoise correction. The results of the calculations are compared with semi-empirical one-, two-, and three-body potentials, and new best estimates of the electronic dissociation energies and barriers are inferred. For $(HF)_2$, $(HF)_3$, $(HF)_4$, and $(HF)_5$, respectively, we obtain for the electronic dissociation energies into monomers 19.1(2), 64(2), 116(3) and 158(4) kJ mol$^{-1}$, and for the electronic barriers to concerted hydrogen exchange 175(10), 85(10), 60(10) and 65(10) kJ mol$^{-1}$. The results are shown to be consistent with NMR line broadening data within the framework of transition state theory.

## 1. Introduction

The thermodynamics and kinetics of the fundamental processes of hydrogen bond dynamics in hydrogen bonded clusters are of wide ranging importance in chemistry, physics and biology. The first step in our theoretical understanding of such processes is provided by a good characterization of the most important parts of the electronic potential hypersurfaces for such systems [1], prototypes being clearly $(HF)_n$. These clusters show rearrangements of the three basic types, illustrated here for the dimer [2, 3]:

(i) Hydrogen bond dissociation

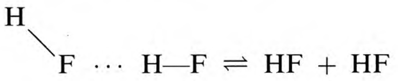
(1)

(ii) Hydrogen bond switching or concerted exchange between bonding and free positions

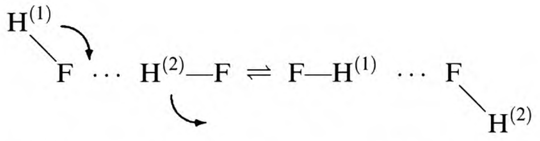
(2)

(iii) Concerted hydrogen exchange between binding sites

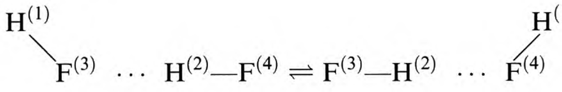
(3)

These processes being exemplified here for the dimer occur in a similar fashion also for larger complexes $(HF)_n$ with $n \geqslant 3$. Whereas at least for the dimer $(HF)_2$ there is considerable experimental and theoretical work available for the first two processes (i) and (ii), little is known about process (iii), and much less is known in general about all three processes in the larger clusters $(HF)_{n\geqslant 3}$ (see [1] and references cited therein). Some initial theoretical work to fill this gap has been carried out recently [4]. It is the aim of the present investigation to provide a more detailed *ab initio* investigation of the important properties of the electronic potential, particularly for the processes (i)

---

[§] Present address: Institut für Physikalische Chemie, Universität Göttingen, Tammannstr. 6, D-37077 Göttingen, Germany.

0026–8976/98 $12·00

and (iii) which are perhaps competitive in the larger clusters $(HF)_n$. In essence we aim for the highest possible level of electronic structure calculation which is currently practical for the $(HF)_n$ system. These results should thus provide a benchmark for simpler theoretical approaches and should also be useful for testing and improving empirical potential hypersurfaces for the larger clusters, somewhat similar in spirit to our investigation on $(HF)_2$ [5].

Cohesion in molecular solids and liquids is often described as a superposition of all individual molecular *pair* interactions, thus neglecting any cooperative effects. For electrostatic forces represented by the Coulomb law between point particles, this would be rigorously true. Given the success of electrostatic models for hydrogen bonding [6], pairwise additive approaches may therefore seem to be quite appropriate for this important class of intermolecular interactions. Hydrogen fluoride (HF) provides an interesting test case. Its charge distribution is highly polar and very compact, with only ten strongly bound electrons and a correspondingly small polarizability. Since important cooperative interaction mechanisms are proportional to the polarizability [7] (induction) or even to its cube [8] (dispersion), one might expect the pairwise additive approximation to be excellent for clusters of this molecule. The opposite is true. Upon aggregation, the molecular charge distribution is significantly distorted. As a consequence, the FH···F bond geometry, energetics, and dynamics vary over a wide range with increasing cluster size [4, 9–19]. Rather than trying to interpret these changes in terms of mechanistic contributions to the hydrogen bond, such as exchange or covalent terms, we will adopt the more formal approach of many-body decomposition. Regarding HF as the building block, we will evaluate which fraction of the total interaction energy can be reduced to pairs, triples, etc. of these molecular units.

A further reason to study hydrogen fluoride is that clusters of four to seven molecules are more abundant in the vapour phase of HF than in any other known gaseous hydrogen bonded system [18] under ordinary pressure and temperature conditions. A remarkable feature of this vapour phase is the coalescence of the $^1H$–$^{19}F$ spin–spin coupling doublet in NMR spectra down to the lowest pressures that have been investigated [20, 21]. This means that beyond rapid cluster dissociation/association processes, there must be an exchange of hydrogen atoms among the fluorine atoms [12, 22] on a microsecond or even shorter timescale [21]. Given the large dissociation energy of monomeric HF ($D_e = 590.5\,\mathrm{kJ\,mol^{-1}}$), more efficient paths have to be present in the clusters. It is now well established by theoretical calculations [4, 12, 19, 22–25] that these pathways involve a concerted cyclic hydrogen exchange, represented schematically as


(4)

for the cyclic HF tetramer. The key quantities for an understanding of these thermodynamic and kinetic anomalies of the HF vapour are cluster dissociation energies $D_e$ and hydrogen exchange barriers $\Delta E$ as a function of size. The main objective of the present study is to compute these quantities by means of a many-body decomposition of the total interaction energy. An optimal coverage of electron correlation contributions in these extended hydrogen bond systems is achieved by using different electronic structure approaches for the various $k$-body terms in the spirit of [16, 26].

## 2. Computational details

### 2.1. *Geometries*

In the present study, we apply a many-body decomposition of the total electronic energy of the HF oligomers [15] and employ different levels of *ab initio* theory and one-particle basis sets to compute the individual many-body terms. The use of a variety of computational methods is a key ingredient of our approach, and there is no fundamental difficulty in computing analytical first and second derivatives of the total energy with respect to the nuclear replacements, as these derivatives can be evaluated separately for each energy that contributes to a given many-body term. Thus, at least in principle, it is straightforward to optimize the geometries or, if desired, to compute the harmonic vibrational frequencies at such a mixed level of theory. At present, however, we have at our disposal neither the computational tools to carry out these optimizations nor, more importantly, the computing resources to do so at the very high levels of calculation that are applied in the present study. Therefore, due to the technical limitations, we concentrate on the computation of the total electronic energy of the HF oligomers at *fixed geometries*. These geometries are sketched in figure 1, and the corresponding geometrical parameters are given in table 1. The geometries correspond to the 'best estimates' derived by Maerker *et al.* [1, 4], except for the minimum energy structure of the trimer, which is taken from table 2 of [1]. This exception was made because the trimer structure of [1] has already served as a point of reference in previous *ab initio* investigations by Tschumper *et al.* [27]. The difference between the two trimer structures of [4] and [1] is so small that it is irrelevant for the purpose of the present study. The structure of [1] is

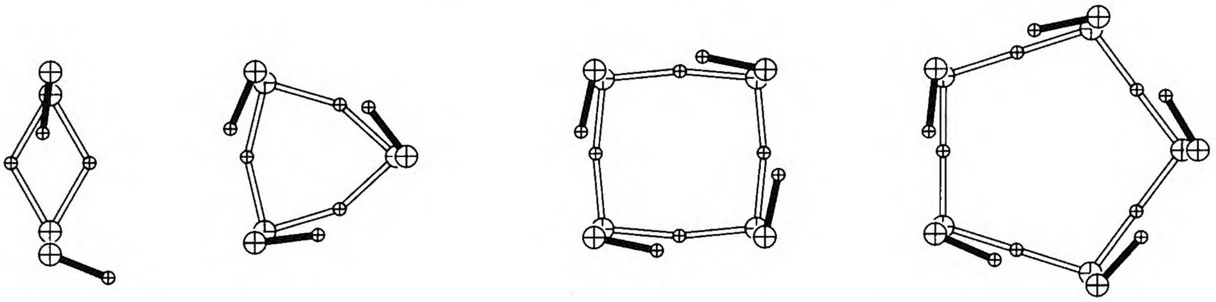

Figure 1. Superimposed representation of the minimum energy structure (upper) and the concerted hydrogen exchange saddle point structure (lower) of the cyclic $(HF)_n$ oligomers ($n = 2, \ldots, 5$). The corresponding geometrical parameters [1, 4] were kept fixed in the present study and are given in table 1.

Table 1. Geometrical parameters of the $(HF)_n$ oligomers. All parameters were kept fixed in the present study. Given are the F–F internuclear separation and the H–F bond length and H–F–F bond angle of the H atom engaged in the hydrogen bond. For the dimer, the H–F bond length and H–F–F bond angle of the 'free' H atom are given in parentheses.

| $n$ | Symmetry | $R_{FF}$/pm | $R_{HF}$/pm | ∠HFF/° |
|---|---|---|---|---|
| (a) Minimum energy structures | | | | |
| 1 | $C_{\infty v}$ | | 91.7 | |
| 2 | $C_s$ | 273.5 | 92.3 (92.0) | 7 (68) |
| 3 | $C_{3h}$ | 257 | 93.3 | 23 |
| 4 | $C_{4h}$ | 251 | 94.4 | 12 |
| 5 | $C_{5h}$ | 248 | 94.8 | 6 |
| (b) Concerted hydrogen exchange saddle points | | | | |
| 2 | $D_{2h}$ | 206 | 118 | |
| 3 | $D_{3h}$ | 224 | 115 | |
| 4 | $D_{4h}$ | 226 | 113.5 | |
| 5 | $D_{5h}$ | 226 | 113 | |

based on semi-empirical one-, two-, and three-body potentials, and is supposed to be rather accurate. Based on the semi-empirical potential energy hypersurface, harmonic vibrational frequencies have been computed [1], and a detailed comparison with corresponding *ab initio* CCSD(T) results is found in [27].

### 2.2. *Many-body decomposition*

The quantity $E^n(k)$, with $k \leqslant n$, is defined as the total (adiabatic) electronic and internuclear energy of the $(HF)_k$ fragment of the oligomer $(HF)_n$ for a given, fixed nuclear structure. This energy is obtained from an *ab initio* calculation of the fragment, taking as nuclear coordinates the positions of the nuclei in the $(HF)_n$ oligomer. In terms of these fragment energies, a many-body decomposition of the total energy can be carried out in the usual manner (cf. [1]). Due to the high point group symmetry of the $(HF)_n$ structures in the present study, the oligomers contain many equivalent fragments, and the $m$-body contributions can be expressed in terms of relatively few fragment energies $E^n(k)$, with $k \leqslant m$. The final expressions are displayed in table 2. Throughout the present study, all fragment energies $E^n(k)$ that contribute to the $m$-body term $V_m$ of the oligomer $(HF)_n$ were computed employing the same basis set for all fragments $(HF)_k$ with $k = 1, \ldots, m$. The basis set used corresponds to the basis of the $(HF)_m$ fragment itself or of the whole $(HF)_n$ oligomer. Any difference between these two choices will vanish in the limit of an infinite basis. Thus, the counterpoise procedure [28] is incorporated automatically in all our calculations, and in the present study, we report only counterpoise corrected $m$-body terms. The basis sets used for the computation of a many-body term $V_m$ are denoted as $(HF)_l$-'basis', where $l \geqslant m$ and 'basis' is either DZP, T/Q, or Q/5 (cf. section 2.4).

The high symmetry of the oligomers cannot be exploited when the calculations are carried out in a basis set of a fragment smaller than the oligomer itself. For example, when the three-body term $V_3$ of the pentamer is computed using for all calculations the basis set of the trimer fragment of interest, the three calculations of the monomer units within the trimer fragment are no longer equivalent because the one-particle basis set is different for the three monomer units. This also applies to the calculation of the dimer fragments within the trimer fragment, and thus, the determination of a three-body term of the pentamer involves seven electronic structure calculations when the trimer fragment basis set is used (1 trimer, 3 dimer, and 3 monomer calculations). Using the whole pentamer basis set, the number of calculations is only four (1 trimer, 2 dimer, and 1 monomer calculations).

We emphasize that a meaningful discussion of many-body contributions to cluster interaction energies

Table 2. Many-body decomposition of the total electronic energy of $(HF)_n$ oligomers in terms of many-body contributions $V_m$, where $E^n(k)$ is the energy of the $(HF)_k$ fragment in the geometry of the $(HF)_n$ oligomer. For the geometries considered in the present study, the dimer contains two different HF monomer fragments (hydrogen bond donor and acceptor, denoted as 1 and 1′), the tetramer contains two different $(HF)_2$ fragments, denoted as 2 and 2′, and the pentamer contains two different $(HF)_2$ as well as two different $(HF)_3$ fragments, denoted as 2/2′ and 3/3′, respectively. The $k'$ fragments refer to structures where one monomer unit is not neighbouring the other monomer unit(s). See also figure 1 of [1].

| $n$ | $V_m$ |
|---|---|
| 2 | $V_1 = E^2(1) + E^2(1') - 2E^1(1)$ |
| | $V_2 = E^2(2) - E^2(1) - E^2(1')$ |
| 3 | $V_1 = 3[E^3(1) - E^1(1)]$ |
| | $V_2 = 3[E^3(2) - 2E^3(1)]$ |
| | $V_3 = E^3(3) - 3E^3(2) + 3E^3(1)$ |
| 4 | $V_1 = 4[E^4(1) - E^1(1)]$ |
| | $V_2 = 4[E^4(2) - 2E^4(1)]$ |
| | $V_2' = 2[E^4(2') - 2E^4(1)]$ |
| | $V_3 = 4[E^4(3) - 2E^4(2) - E^4(2') + 3E^4(1)]$ |
| | $V_4 = E^4(4) - 4E^4(3) + 4E^4(2) + 2E^4(2') - 4E^4(1)$ |
| 5 | $V_1 = 5[E^5(1) - E^1(1)]$ |
| | $V_2 = 5[E^5(2) - 2E^5(1)]$ |
| | $V_2' = 5[E^5(2') - 2E^5(1)]$ |
| | $V_3 = 5[E^5(3) - 2E^5(2) - E^5(2') + 3E^5(1)]$ |
| | $V_3' = 5[E^5(3') - E^5(2) - 2E^5(2') + 3E^5(1)]$ |
| | $V_4 = 5[E^5(4) - 2E^5(3) - 2E^5(3') + 3E^5(2) + 3E^5(2') - 4E^5(1)]$ |
| | $V_5 = E^5(5) - 5E^5(4) + 5E^5(3) + 5E^5(3') - 5E^5(2) - 5E^5(2') + 5E^5(1)$ |

requires realistic and uniform geometries due to the strong dependence of these contributions on the cluster structure. Comparison of dimer-derived geometries [29] or among different minimum structures for various electronic structure levels [30] are less useful.

Finally, the many-body decomposition of the total electronic energy of the oligomers is not completely straightforward for the concerted hydrogen exchange saddle points. In these structures, the monomer fragments lose their identity. Nevertheless, we decompose the energies in the same manner as for the equilibrium structures. This would not be a problem, if the structure is displaced infinitesimally from the symmetric structure, anyway.

### 2.3. *Electronic structure calculations*

The main objective of the present work is to compute the electronic dissociation energies $D_e$ and the barriers to concerted hydrogen exchange $\Delta E$ as close as technically possible to the limit of a complete one-particle basis set, preferably to the highest level of electronic structure calculations that is currently available and affordable.

For the one- and two-body terms, we employ the CCSD(T)-R12 method. This method is identical to the usual CCSD(T) model, but exploits many-electron basis functions that depend explicitly on the interelectronic coordinates $r_{ij}$. In contrast to the CCSD(T)-R12 method, conventional *ab initio* calculations employ many-electron basis functions that consist of (antisymmetrized) products of one-electron orbitals. The explicitly $r_{ij}$-dependent basis functions solve the interelectronic cusp problem, and yield a significantly improved convergence to the limit of a complete one-particle basis set for the computed energy. The CCSD(T)-R12 theory, as developed by Noga, Klopper and Kutzelnigg [31–34], has been applied very recently in the framework of benchmark coupled cluster calculations of the ten-electron systems $CH_5^+$ [35] and $H_2O$ [36], demonstrating its great potential with respect to the quantitatively accurate computation of absolute energies.

For the three-body terms, we employ the *conventional* CCSD(T) method, that is, without explicit $r_{ij}$-dependence. Using an aug-cc-pVTZ/aug-cc-pVQZ-type basis set, these calculations represent presumably the most accurate level of *ab initio* theory that can be applied today for the computation of the three-body terms.

Finally, for the four- and five-body terms, we employ explicitly correlated second-order Møller–Plesset perturbation theory (MP2-R12) using the same aug-cc-pVTZ/aug-cc-pVQZ-type basis set.

The 1s core orbitals of the F atoms were not correlated in any of the electron correlation treatments applied in the present work. This is in contrast to previous MP2/DZP calculations, where the core orbitals were included [16].

The SCF calculations of all fragments up to the pentamer were performed with the `SORE` program [37] on the Cray Origin 2000 of the University of Bergen. Subsequently, this program was run on the NEC SX-4 supercomputer of the Swiss Center for Scientific Computing (CSCS/SCSC) to provide the corresponding MP2 and MP2-R12 second-order correlation energies. The CCSD(T)-R12 calculations of the monomer and dimer fragments were carried out with the `DIRCCR12-95` program [38] on the IBM RS/6000 workstations cluster of the University of Oslo. The conventional CCSD(T) calculations using the T/Q basis set (see section 2.4) of the dimer and trimer fragments were performed with the `Gaussian 94` program [39] on the NEC SX-4 of the CSCS/SCSC computing centre. The corresponding calculations of the monomer fragments as well as all calculation with the DZP basis set were obtained with the same program on the DEC 8400 5/300 Alpha servers of the ETH Zürich ($C^4$ project).

### 2.4. *Basis sets*

Three basis sets have been used in the present study. The first basis set is the DZP basis set that was used in previous calculations of the three-body potential of $(HF)_n$ clusters [1, 16]. These calculations led to the HF3BG potential, which is an anaytical fit to about 3000 counterpoise corrected MP2/DZP points, without further adjustments [1].

The second basis set is the aug-cc-pV(T/Q)Z basis set (abbreviated as T/Q) that was used in previous calculations of the two-body potential [5]. Employing this basis set, counterpoise corrected MP2-R12 calculations were performed for 3284 points on the six-dimensional hypersurface of the HF dimer. Applying empirical adjustments, the analytical two-body potentials SC-2.9 and SO-3 were derived [5, 40].

The third basis set has been constructed for the present CCSD(T)-R12 study. It is denoted as aug-cc-pV(Q/5)Z basis (abbreviated as Q/5), and has been constructed in analogy with the T/Q basis. The Q/5 basis set for the F atom is 15s9p4d3f2g contracted to 10s7p4d3f2g. The s- and p-type primitive functions were taken from the aug-cc-pV5Z basis and contracted to 10s7p by the segmented contraction scheme (6111111111) for s and (3111111) for p, using the contraction coefficients of the innermost aug-cc-pV5Z orbitals. The 4d3f2g polarization functions were taken from the aug-cc-pVQZ basis. The Q/5 basis set for the H atom is 9s4p3d2f contracted to 7s4p3d2f. The s-type primitive functions were taken from the aug-cc-pV5Z basis and contracted to 7s by the segmented contraction scheme (3111111). The 4p3d2f set was taken from the aug-cc-pVQZ basis.

For completeness, the exponents and contraction coefficients of the three basis sets are given in table 3. All the parameters of the aug-cc-pVXZ $(X = T, Q, 5)$ basis sets [41–43] were downloaded from the EMSL basis set database [44]. Only the pure spherical harmonic components of the basis functions (5d, 7f and 9g) were used in the calculations carried out in the course of the present work. Note that in our previous MP2/DZP calculations, six d-components were used [16].

As noted before, the fragment basis sets are denoted as $(HF)_l$-'basis'. For example, the $(HF)_3$-DZP basis set contains 60, the $(HF)_3$-T/Q basis set contains 228, the $(HF)_2$-Q/5 basis set contains 276, and the $(HF)_5$-T/Q basis set contains 380 basis functions.

## 3. Results

Table 4 displays the computed many-body decomposition of the total energy of the $(HF)_n$ oligomers for the minimum energy structures (a) and the concerted hydrogen exchange saddle points (b). This table collects our most accurate results, which are compared with the semi-empirical one- and two-body potentials [40] and the analytical fit (HF3BG) to the MP2/DZP-level three-body terms [16].

The CCSD(T)-R12/HF-Q/5 calculations of the one-body or monomer relaxation [45, 46] term agree excellently with the generalized Pöschl–Teller (GPT) monomer potential [40]. For the minimum energy structures, the difference between the *ab initio* computations and the GPT values is not larger than 0.05 kJ mol$^{-1}$ per HF monomer fragment, and for the saddle points, this difference is not larger than 0.1 kJ mol$^{-1}$ per fragment. It is very satisfactory to find that the CCSD(T)-R12 calculations describe the monomer potential so accurately, especially in view of the substantial HF bond elongation (by 20–25%) in the saddle point stuctures.

Concerning the two-body term, it is apparent that the semi-empirical SO-3 potential cannot be used to describe the two-body term of the saddle point structures. The very short FF distances in these structures lie outside the range of distances where the potential is valid. In contrast, the two-body terms $V_2'$ for the interaction between two non-neighbouring monomer fragments as present in the tetramer and pentamer agree well with the *ab initio* calculations, as do the SO-3 values for the minimum energy structures. Comparison of the MP2-R12, CCSD(T)-R12 and SO-3 results for $V_2$ in table 4, part (a) suggests that the empirical modification of the SO-3 potential relative to the raw MP2-R12 *ab initio* potential is generally a refinement in the vicinity of the minimum energy structures. In conclusion, the SO-3 potential can be employed to describe the minimum energy structures, but not the saddle points. For the dimer the range of validity is expected to extend to about 100 kJ mol$^{-1}$ above the minimum, still far below the exchange saddle point in this case. For the higher oligomers, the range of validity is restricted to even smaller *total* energies for some hydrogen exchange configurations.

Similar conclusions can be inferred from the comparison of the three-body terms. The HF3BG fit [16] of the MP2/DZP calculations fails for the saddle point structures, as no configurations near these structures had been incorporated into the fitting procedure. This is due to fundamental limitations of the current analytical $V_2, V_3$ expressions for situations where chemical bonds and hydrogen bonds are of comparable length [1]. In fact, the analytical surfaces are by design too repulsive in this situation, so that adiabatic symmetrization schemes [1, 47] can in principle be applied for refinement. In contrast, the inaccuracy of the HF3BG fit for the relatively small $V_3'$ three-body term (where one monomer fragment is not neighbouring the other two) of the minimum energy structure of $(HF)_5$ is within the expected error bars of the analytical fit (which has a rms deviation of 1.8 kJ mol$^{-1}$, to be multiplied by 5 due to

Table 3. Gaussian basis sets used in the present study. $\zeta$ is the exponent of the basis function and $c$ is the coefficient of the segmented contraction of the normalized primitive Gaussians.

| | s | | p | | d | f | g |
|---|---|---|---|---|---|---|---|
| | $\zeta$ | $c$ | $\zeta$ | $c$ | $\zeta$ | $\zeta$ | $\zeta$ |
| | | | DZP | | | | |
| Fluorine | 9 994.790 | 0.002 017 | 44.355 50 | 0.020 868 | 1.200 000 | | |
| | 1 506.030 | 0.015 295 | 10.082 00 | 0.130 092 | | | |
| | 350.269 0 | 0.073 110 | 2.995 900 | 0.396 219 | | | |
| | 104.053 0 | 0.246 420 | 0.938 300 | 0.620 368 | | | |
| | 34.843 20 | 0.612 593 | 0.273 300 | | | | |
| | 4.368 800 | 0.242 489 | | | | | |
| | 12.216 40 | | | | | | |
| | 1.207 800 | | | | | | |
| | 0.363 400 | | | | | | |
| | | | T/Q | | | | |
| | 74 530.00 | 0.000 095 | 80.390 00 | 0.006 347 | 3.107 000 | 1.917 000 | |
| | 111 70.00 | 0.000 738 | 18.630 00 | 0.044 204 | 0.855 000 | 0.724 000 | |
| | 2 543.000 | 0.003 858 | 5.694 000 | 0.168 514 | 0.292 000 | | |
| | 721.000 0 | 0.015 926 | 1.953 000 | | | | |
| | 235.900 0 | 0.054 289 | 0.670 200 | | | | |
| | 85.600 00 | 0.149 513 | 0.216 600 | | | | |
| | 33.550 00 | | 0.065 680 | | | | |
| | 13.930 00 | | | | | | |
| | 5.915 000 | | | | | | |
| | 1.843 000 | | | | | | |
| | 0.712 400 | | | | | | |
| | 0.263 700 | | | | | | |
| | 0.085 940 | | | | | | |
| | | | Q/5 | | | | |
| | 211 400.0 | 0.000 026 | 241.900 0 | 0.001 002 | 5.014 000 | 3.562 000 | 2.376 000 |
| | 31 660.00 | 0.000 201 | 57.170 00 | 0.008 054 | 1.725 000 | 1.148 000 | 0.924 000 |
| | 7 202.000 | 0.001 056 | 18.130 00 | 0.038 048 | 0.586 000 | 0.460 000 | |
| | 2 040.000 | 0.004 432 | 6.624 000 | | 0.207 000 | | |
| | 666.400 0 | 0.015 766 | 2.622 000 | | | | |
| | 242.000 0 | 0.048 112 | 1.057 000 | | | | |
| | 95.530 00 | | 0.417 600 | | | | |
| | 40.230 0 | | 0.157 400 | | | | |
| | 17.720 00 | | 0.055 000 | | | | |
| | 8.005 000 | | | | | | |
| | 3.538 000 | | | | | | |
| | 1.458 000 | | | | | | |
| | 0.588 700 | | | | | | |
| | 0.232 400 | | | | | | |
| | 0.080 600 | | | | | | |
| | | | DZP | | | | |
| Hydrogen | 19.240 60 | 0.032 828 | 1.000 000 | | | | |
| | 2.899 200 | 0.231 208 | | | | | |
| | 0.653 400 | 0.817 238 | | | | | |
| | 0.177 600 | | | | | | |
| | | | T/Q | | | | |
| | 82.640 00 | 0.002 006 | 1.407 000 | | 1.057 000 | | |
| | 12.410 00 | 0.015 343 | 0.388 000 | | 0.247 000 | | |
| | 2.824 000 | 0.075 579 | 0.102 000 | | | | |
| | 0.797 700 | | | | | | |
| | 0.258 100 | | | | | | |
| | 0.089 890 | | | | | | |
| | 0.023 630 | | | | | | |
| | | | Q/5 | | | | |
| | 402.000 0 | 0.000 279 | 2.292 000 | | 2.062 000 | 1.397 000 | |
| | 60.240 00 | 0.002 165 | 0.838 000 | | 0.662 000 | 0.360 000 | |
| | 13.730 00 | 0.011 201 | 0.292 000 | | 0.190 000 | | |
| | 3.905 000 | | 0.084 800 | | | | |
| | 1.283 000 | | | | | | |
| | 0.465 500 | | | | | | |
| | 0.181 100 | | | | | | |
| | 0.072 790 | | | | | | |
| | 0.020 700 | | | | | | |

Table 4. Computed and semi-empirical $m$-body contributions $V_m$ to the electronic dissociation energy for minimum (a) and saddle point structures (b) with respect to fragmentation of $(HF)_n$ oligomers into separate monomers. The two- and three-body terms are decomposed into two contributions: $V_2/V_3$ from structures with neighbouring monomer units, and $V_2'/V_3'$ from structures where one of the monomer units is not neighbouring the other(s). All energies are given in kJ mol$^{-1}$.

| $V_m$ | $n=2$ | $n=3$ | $n=4$ | $n=5$ | Method | Basis[a] |
|---|---|---|---|---|---|---|
| (a) Minimum energy structures | | | | | | |
| $V_1$ | 0.11 | 2.07 | 7.79 | 12.75 | CCSD(T)-R12 | HF-Q/5 |
| | 0.13 | 2.17 | 7.98 | 13.02 | GPT[b] | |
| $V_2$ | −19.07 | −50.21 | −64.21 | −70.99 | CCSD(T)-R12 | $(HF)_2$-Q/5 |
| | −19.21 | −51.66 | −66.89 | −74.96 | SO-3[c] | |
| | −18.22 | −46.74 | −60.25 | −66.63 | MP2-R12 | $(HF)_n$-T/Q |
| $V_2'$ | | | −14.47 | −26.09 | CCSD(T)-R12 | $(HF)_2$-Q/5 |
| | | | −16.06 | −26.24 | SO-3[c] | |
| | | | −15.17 | −26.09 | MP2-R12 | $(HF)_n$-T/Q |
| $V_3$ | | −14.66 | −38.98 | −52.02 | CCSD(T) | $(HF)_3$-T/Q |
| | | −14.98 | −36.86 | −53.39 | HF3BG[d] | |
| $V_3'$ | | | | −10.53 | CCSD(T) | $(HF)_3$-T/Q |
| | | | | −4.95 | HF3BG[d] | |
| $V_4$ | | | −3.60 | −8.43 | MP2-R12 | $(HF)_n$-T/Q |
| $V_5$ | | | | −0.66 | MP2-R12 | $(HF)_n$-T/Q |
| (b) Concerted hydrogen exchange saddle points | | | | | | |
| $V_1$ | 225.80 | 282.22 | 339.56 | 409.35 | CCSD(T)-R12 | HF-Q/5 |
| | 225.59 | 282.27 | 339.78 | 409.68 | GPT[b] | |
| $V_2$ | −66.72 | −31.28 | −8.66 | 13.65 | CCSD(T)-R12 | $(HF)_2$-Q/5 |
| | 101.08 | 12.53 | 21.02 | 48.37 | SO-3[c] | |
| | −72.02 | −40.08 | −17.90 | 2.73 | MP2-R12 | $(HF)_n$-T/Q |
| $V_2'$ | | | −35.21 | −55.99 | CCSD(T)-R12 | $(HF)_2$-Q/5 |
| | | | −32.64 | −51.29 | SO-3[c] | |
| | | | −36.12 | −57.77 | MP2-R12 | $(HF)_n$-T/Q |
| $V_3$ | | −226.35 | −310.39 | −318.95 | CCSD(T) | $(HF)_3$-T/Q |
| | | −105.28 | −263.72 | −313.62 | HF3BG[d] | |
| $V_3'$ | | | | −58.31 | CCSD(T) | $(HF)_3$-T/Q |
| | | | | −25.92 | HF3BG[d] | |
| $V_4$ | | | −35.05 | −75.08 | MP2-R12 | $(HF)_n$-T/Q |
| $V_5$ | | | | −0.54 | MP2-R12 | $(HF)_n$-T/Q |

[a] The notation $(HF)_n$-'basis' indicates that the particular $m$-body term is obtained from a series of calculations of different fragments that all use the composite basis set of the whole $(HF)_n$ oligomer, centred as its coordinates.

[b] Generalized Pöschl–Teller oscillator [5, 40].

[c] Semi-empirical pair potential [5, 40].

[d] Three-body term fitted to MP2/DZP results [16].

the fivefold occurrence of the *same* three-body interaction in $V_3'$ of $(HF)_5$).

To gain insight into the basis set effects, second-order correlation effects, and higher-order correlation effects on the three-, four-, and five-body terms, we have computed these many-body terms using the DZP and T/Q basis sets in the framework of the SCF, MP2, and CCSD(T) methods. The results of these calculations are collected in table 5, and can be used to assess the accuracy or reliability of the three- and higher-body terms in table 4.

For the three-body term of the tetramer and pentamer, we have employed either the basis set of the trimer fragment of interest for all the calculations of this particular fragment and subfragments (denoted as $(HF)_3$-DZP or -T/Q), or the basis set of the whole $(HF)_n$ oligomer (denoted as $(HF)_n$-DZP or -T/Q). For the T/Q basis set, the differences between the results obtained with the $(HF)_3$- and $(HF)_n$-type basis sets are very small, with a maximum for the saddle points of *ca.* 0.4 kJ mol$^{-1}$ at the MP2 level, but for the DZP basis set, we observe relatively large differences, up to

Table 5. Comparison of three-, four-, and five-body contributions obtained from different methods and basis sets. The term $V_3'$ denotes the three-body contribution from a structure where one monomer unit is not neighbouring the other two units. All energies are given in kJ mol$^{-1}$.

| | | $n = 3$ | $n = 4$ | $n = 4$ | $n = 5$ | $n = 5$ | $n = 5$ | $n = 5$ |
|---|---|---|---|---|---|---|---|---|
| Method | Basis[a] | $V_3$ | $V_3$ | $V_4$ | $V_3$ | $V_3'$ | $V_4$ | $V_5$ |
| (a) Minimum energy structures | | | | | | | | |
| SCF | $(HF)_3$-DZP | −13.48 | −37.39 | | −52.05 | −9.47 | | |
| MP2 | $(HF)_3$-DZP | −14.49 | −39.04 | | −53.77 | −9.52 | | |
| CCSD(T) | $(HF)_3$-DZP | −14.44 | −38.98 | | −53.85 | −9.46 | | |
| SCF | $(HF)_n$-DZP | −13.48 | −38.83 | −2.72 | −52.60 | −10.30 | −6.56 | −0.40 |
| MP2 | $(HF)_n$-DZP | −14.49 | −40.30 | −3.22 | −54.67 | −10.76 | −7.71 | −0.54 |
| CCSD(T) | $(HF)_n$-DZP | −14.44 | −40.27 | −3.32 | −54.78 | −10.68 | −7.87 | −0.57 |
| SCF | $(HF)_3$-T/Q | −14.43 | −38.79 | | −52.09 | −10.60 | | |
| MP2 | $(HF)_3$-T/Q | −14.86 | −39.18 | | −51.90 | −10.66 | | |
| CCSD(T) | $(HF)_3$-T/Q | −14.66 | −38.98 | | −52.02 | −10.53 | | |
| SCF | $(HF)_n$-T/Q | −14.43 | −38.83 | −3.16 | −52.12 | −10.63 | −7.44 | −0.51 |
| MP2 | $(HF)_n$-T/Q | −14.86 | −39.24 | −3.63 | −51.96 | −10.73 | −8.50 | −0.66 |
| MP2-R12 | $(HF)_n$-T/Q | −14.83 | −39.17 | −3.60 | −51.89 | −10.73 | −8.43 | −0.66 |
| (b) Concerted hydrogen exchange saddle points | | | | | | | | |
| SCF | $(HF)_3$-DZP | −239.05 | −324.86 | | −343.64 | −57.79 | | |
| MP2 | $(HF)_3$-DZP | −237.18 | −322.06 | | −335.87 | −55.91 | | |
| CCSD(T) | $(HF)_3$-DZP | −244.72 | −330.15 | | −344.10 | −56.02 | | |
| SCF | $(HF)_n$-DZP | −239.05 | −330.74 | −32.66 | −347.73 | −62.14 | −68.31 | 0.11 |
| MP2 | $(HF)_n$-DZP | −237.18 | −331.08 | −34.68 | −342.75 | −62.45 | −77.61 | 1.19 |
| CCSD(T) | $(HF)_n$-DZP | −244.72 | −339.43 | −36.26 | −351.16 | −62.45 | −81.64 | 1.60 |
| SCF | $(HF)_3$-T/Q | −230.08 | −315.66 | | −329.05 | −60.18 | | |
| MP2 | $(HF)_3$-T/Q | −219.80 | −302.98 | | −310.82 | −58.36 | | |
| CCSD(T) | $(HF)_3$-T/Q | −226.35 | −310.39 | | −318.95 | −58.31 | | |
| SCF | $(HF)_n$-T/Q | −230.08 | −315.82 | −33.42 | −329.21 | −60.29 | −68.37 | −0.93 |
| MP2 | $(HF)_n$-T/Q | −219.80 | −303.38 | −35.37 | −311.24 | −58.65 | −75.93 | −0.51 |
| MP2-R12 | $(HF)_n$-T/Q | −218.69 | −302.35 | −35.05 | −310.56 | −58.63 | −75.08 | −0.54 |

[a] The notation $(HF)_3$-'basis' indicates that the three-body term is obtained from calculations using the basis set of the corresponding $(HF)_3$ fragment that is part of the $(HF)_n$ oligomer.

1.3 kJ mol$^{-1}$ for the minimum energy structures and up to ≈10 kJ mol$^{-1}$ for the saddle points.

A comparison of the DZP and T/Q results reveals that the four- and five-body terms are not very sensitive to the quality of the basis set, neither for the minimum energy structures, nor for the saddle points. The effects are of the order of 1–2 kJ mol$^{-1}$. This is in sharp contrast to the three-body term, in particular for the saddle point structures. For these structures, for example, the CCSD(T) values obtained from the two different basis sets differ by as much as 20–30 kJ mol$^{-1}$.

The difference between the MP2 and CCSD(T) values is very small for the many-body terms of the minimum energy structures. For the saddle point structures, however, the magnitude of the $V_3$ terms increases by as much as 7–8 kJ mol$^{-1}$ from MP2 to CCSD(T). Interestingly, exactly the same increase due to higher-order correlation effects is observed for both basis sets, indicating that this effect is not very basis set dependent. A moderate increase in magnitude with higher order correlation contributions is also found for the $V_4$ terms.

Based on the above observations, we conclude the following: first, the three-body terms of the minimum energy structures computed at the CCSD(T)/$(HF)_3$-T/Q level are accurate to within 1 kJ mol$^{-1}$, or perhaps 2 kJ mol $^{-1}$ for the pentamer. Second, noting the small difference between the MP2 and CCSD(T) results for the four- and five-body terms of the minimum energy structures at the DZP level, we conclude that the MP2-R12/$(HF)_n$-T/Q values are our most accurate four- and five-body terms, probably to within 1 kJ mol$^{-1}$. Third, the accuracy of the three-body terms of the saddle point structures remains quite uncertain. It appears that these terms, which are up to an order of magnitude larger than the pair attractions, are the most critical contributions. Owing to their uncertainty, we will not be able to reduce the error bars on our previous best estimates of the barrier to concerted hydrogen exchange significantly below 10 kJ mol$^{-1}$ [4].

Table 6. Electronic dissociation energies and barriers to concerted hydrogen exchange of cyclic $(\mathrm{HF})_n$ oligomers ($n = 2, \ldots, 5$). All energies in kJ mol$^{-1}$. The dissociation energies in the upper part of the table refer to fragmentation into monomers. Stepwise dissociation energies can be obtained as the difference between adjacent $D_e$ values and are explained and shown in figure 2. The values in brackets [...] do not include the four- and five-body terms and correspond to relaxed geometries in the respective potential.

| | | | | |
|---|---|---|---|---|
| (a) Electronic dissociation energy | | | | |
| SQSBDE\|HF3BG [3, 16, 48] | 18.7 | 61.3 | [113.6] | [152.9] |
| GPT\|SC-2.9\|HF3BG [1] | 19.1 | 64.3 | [111.6] | [147.0] |
| GPT\|SO-3\|HF3BG | 19.1 | 64.5 | [112.0] | [147.4] |
| B3LYP/6-311 + +G(3df, 3pd) [4] | 20.2 | 66.3 | 125.6 | 173.5 |
| MP2/6-311 + +G(3df, 3pd) [4] | 20.7 | 64.7 | 121.7 | 168.1 |
| MP2/[8s6p2d/6s3p] [16] | | 60.9 | | |
| MP2/aug-cc-pV(T/Q)Z[a] | 18.8 | 61.4 | 114.6 | 158.1 |
| | 17.8[b] | 58.3[b] | 108.6[b] | 149.0[b] |
| CCSD(T)/aug-cc-pV(T/Q)Z[a] | 19.2 | 62.8 | | |
| | 18.2[b] | 59.8[b] | | |
| CPF/[3s2p1d/3s1p] [23] | 20.8 | 64.6 | 120.8 | |
| CCSD(T)/[4s3p2d1f/3s2p1d] [24] | | 60.2 | | |
| 'QCISD(T)/6-311+G(3df, 2p)' [49] | 20.5 | 65.8 | | |
| CCSD(T)/TZ2P(f, d) [50] | 19.8 | | | |
| CCSD(T)/TZ2P(f, d) [27] | 20.7 | 67.9 | | |
| CCSD(T)/aug-cc-pVQZ [51] | 19.7 | | | |
| | 18.8[b] | | | |
| CCSD(T)/aug-cc-pVTZ [52] | | 66.2 | | |
| | | 60.1[b] | | |
| Extrapolated CCSD(T) limit [51] | 19.2 | | | |
| $D_e$ (*ab initio*),[c] present work[b] | 19.0 | 62.8 | 113.5 | 156.0 |
| $D_e$ (semi-empirical),[d] present work[b] | 19.1 | 64.2 | 117.6 | 159.8 |
| Previous best estimate [1, 4, 5] | 19.1(2) | 63(3) | 117(4) | 161(5) |
| New estimate, present work | 19.1(2) | 64(2) | 116(3) | 158(4) |
| (b) Barrier to concerted hydrogen exchange | | | | |
| B3LYP/6-311 + +G(3df, 3pd) [4] | 157.8 | 69.6 | 43.6 | 40.8 |
| MP2/6-311 + +G(3df, 3pd) [19] | 167.4 | 78.2 | 53.1 | 52.7 |
| MP2/aug-cc-pV(T/Q)Z[a] | 169.1 | 77.3 | 51.6 | 52.9 |
| | 173.7[b] | 85.2[b] | 61.4[b] | 64.3[b] |
| CCSD(T)/aug-cc-pV(T/Q)Z[a] | 176.8 | 84.6 | | |
| | 180.9[b] | 91.9[b] | | |
| CPF/[3s2p1d/3s1p] [23] | 185 | 86.6 | 61.9 | |
| CCSD(T)/[4s3p2d1f/3s2p1d] [24] | | 75.3 | | |
| CCSD(T)/aug-cc-pVTZ [52] | | 81.9 | | |
| 'QCISD(T)/6-311+G(3df, 2p)' [49] | 186.4 | 95.4 | | |
| CCSD(T)/6-311+G** [4] | | 102.0 | 75.8 | |
| $\Delta E$ (*ab initio*),[e] present work[b] | 178.0 | 87.4 | 63.7 | 70.1 |
| Previous best estimate [1, 4, 5] | 170(10) | 80(10) | 55(10) | 50(10) |
| New estimate, present work | 175(10) | 85(10) | 60(10) | 65(10) |

[a] With respect to the fixed geometries of table 1.

[b] Corrected for the BSSE by the counterpoise procedure.

[c] $D_e\,(\textit{ab initio}) = -(V_{1,2,2'}[\mathrm{CCSD(T)\text{-}R12/(HF)_{1,2}\text{-}Q/5}] + V_{3,3'}[\mathrm{CCSD(T)/(HF)_3\text{-}T/Q}] + V_{4,5}[\mathrm{MP2\text{-}R12/(HF)}_n\text{-}\mathrm{T/Q}])$.

[d] $D_e\,(\text{semi-empirical}) = -(V_1[\mathrm{GPT}] + V_{2,2'}[\mathrm{SO\text{-}3}] + V_{3,3'}[\mathrm{CCSD(T)/(HF)_3\text{-}T/Q}] + V_{4,5}[\mathrm{MP2\text{-}R12/(HF)}_n\text{-}\mathrm{T/Q}])$.

[e] $\Delta E = \Delta V_{1,2,2'}[\mathrm{CCSD(T)\text{-}R12/(HF)_{1,2}\text{-}Q/5}] + \Delta V_{3,3'}[\mathrm{CCSD(T)/(HF)_3\text{-}T/Q}] + \Delta V_{4,5}[\mathrm{MP2\text{-}R12/(HF)}_n\text{-}\mathrm{T/Q}]$.

## 4. Discussion

### 4.1. *Dissociation energies*

Our final results for the potential energies of the relevant high energy stationary points with respect to global minima are displayed in table 6. The electronic dissociation energies ($D_e$) computed in the present study are compared with other *ab initio* calculations and with our previous best estimates of $D_e = 19.1(2)\,\mathrm{kJ\,mol^{-1}}$ for the dimer, $D_e = 63(3)\,\mathrm{kJ\,mol^{-1}}$ for the trimer, $D_e = 117(4)\,\mathrm{kJ\,mol^{-1}}$ for the tetramer, and $D_e = 161(5)\,\mathrm{kJ\,mol^{-1}}$ for the pentamer [1, 4].

Concerning the HF dimer, there is little doubt that the value obtained from the analytical GPT|SO-3 potential is very close (i.e. within $0.2\,\mathrm{kJ\,mol^{-1}}$) to the true electronic dissociation energy. Our GPT|SO-3 value is consistent with the CCSD(T) limit of $19.2\,\mathrm{kJ\,mol^{-1}}$ extrapolated by Peterson and Dunning [51] and with the corresponding CCSD(T)-R12/$(HF)_2$-Q/5 value of $19.0\,\mathrm{kJ\,mol^{-1}}$. With respect to the *ab initio* calculations we note that it is crucial to employ the counterpoise procedure to avoid spurious BSSE effects. The *un*corrected *ab initio* calculations in table 6 yield a much too large $D_e$ ranging from 19.7 to $20.8\,\mathrm{kJ\,mol^{-1}}$. Considering the BSSE, it is worth noting that the two almost identical CCSD(T)/TZ2P(f,d) calculations of [50] and [27] differ by as much as $0.9\,\mathrm{kJ\,mol^{-1}}$ for $D_e$. This difference is mainly due to the calculations of [50] having been performed in a basis set that included all Cartesian components of the basis functions (6d, 10f), whereas the calculations of [27] employed only the spherical harmonic components (5d, 7f). It appears that the BSSE due to the spherical harmonic basis set ($\approx 2.5\,\mathrm{kJ\,mol^{-1}}$) is roughly $1\,\mathrm{kJ\,mol^{-1}}$ larger than for the basis set with Cartesian components ($\approx 1.5\,\mathrm{kJ\,mol^{-1}}$). In view of the BSSE, we also note that the counterpoise correction for the aug-cc-pVQZ basis set amounts to $1.0\,\mathrm{kJ\,mol^{-1}}$ [51]. Thus, the *corrected* CCSD(T)/aug-cc-pVQZ result is $D_e = 18.8\,\mathrm{kJ\,mol^{-1}}$, about $0.3\,\mathrm{kJ\,mol^{-1}}$ below the estimated limit [51]. These findings confirm that BSSE and other basis set incompleteness effects remains a challenge for traditional correlated treatments of hydrogen bonded systems [53].

For the HF trimer, we have computed an electronic dissociation energy of $D_e$ (*ab initio*) $= 62.8\,\mathrm{kJ\,mol^{-1}}$. As the magnitude of the computed two-body interaction is about $1.5\,\mathrm{kJ\,mol^{-1}}$ smaller than the value obtained from the SO-3 potential (cf. table 4, part (a)), the computed value might be too low by a similar amount. We may safely assume that the *ab initio* computed dissociation energy represents a *lower bound* to the true limit, not only for the trimer, but also for the other oligomers, including the dimer. Thus, assuming that the CCSD(T)-R12/$(HF)_2$-Q/5 level of theory still underestimates the magnitude of the pair interaction by a few per cent, we obtain a very realistic value of $D_e(\text{semi-empirical}) = 64.2\,\mathrm{kJ\,mol^{-1}}$ by replacing the CCSD(T)-R12/$(HF)_2$-Q/5 one- and two-body terms by the GPT|SO-3 potential. In any case, both results are well within the uncertainty of the previous best estimate of $D_e = 63 \pm 3\,\mathrm{kJ\,mol^{-1}}$. From the present calculations, we infer a new estimate of $D_e = 64 \pm 2\,\mathrm{kJ\,mol^{-1}}$, which is only a small change with respect to our previous estimate. This value is also in good agreement with an unpublished geometry minimization at CCSD(T)/aug-cc-pVTZ level [52], which yields $60.1\,\mathrm{kJ\,mol^{-1}}$ with and $66.2\,\mathrm{kJ\,mol^{-1}}$ without counterpoise correction. Based partly on a fortuitous cancellation of the BSSE and (other) basis set truncation errors, the results of the other *ab initio* calculations displayed in table 6 are close to our new estimate. Only the CCSD(T) value of 60.2 $\mathrm{kJ\,mol^{-1}}$ obtained by Kormonicki *et al.* [24] is surprisingly low. These authors employed a [4s3p2d1f/3s2p1d] basis set of atomic natural orbitals (ANO). If we were to correct their value for the BSSE by means of the counterpoise correction, the dissociation energy would be reduced further, notably by more than $6\,\mathrm{kJ\,mol^{-1}}$ [24]. Thus, the corresponding counterpoise corrected CCSD(T)/[4s3p2d1f/3s2p1d] value would be in error by about $10\,\mathrm{kJ\,mol^{-1}}$ or roughly 20%. As already anticipated by Komornicki *et al.*, this large error is presumably due to the lack of an appropriate augmentation of the ANO basis set.

Our previous estimates of the dissociation energies of the HF tetramer ($117(4)\,\mathrm{kJ\,mol^{-1}}$) and pentamer ($161(5)$ $\mathrm{kJ\,mol^{-1}}$) are well confirmed by the present caculations (113.5–117.6 and $156.0$–$159.9\,\mathrm{kJ\,mol^{-1}}$, respectively), and there is little reason to revise these estimates. Nevertheless, we infer new estimates of 116(3) for the tetramer and $158(4)\,\mathrm{kJ\,mol^{-1}}$ for the pentamer. Again, previous *ab initio* calculations [4, 23] yielded too large dissociation energies. The contribution of four- and five-body terms to the binding energy of $(HF)_4$ and $(HF)_5$ is notable, but smaller than (and opposed to) the contribution from monomer non-rigidity ($V_1$).

If we take a best estimate of the anharmonic zero point energy difference between $(HF)_4$ and 4 HF of about $29(2)\,\mathrm{kJ\,mol^{-1}}$ [16] and combine this with the experimental bounds for dissociation of a single HF from $(HF)_4$ ($\Delta D_0 = 42$–$43\,\mathrm{kJ\,mol^{-1}}$) [18], for dissociation of a single HF from $(HF)_3$ ($\Delta D_0 = 29$–$32$ $\mathrm{kJ\,mol^{-1}}$) [54], and for dissociation of $(HF)_2$ ($D_0 = 12.70(2)\,\mathrm{kJ\,mol^{-1}}$) [55], all in the sense of equation (1), we obtain $D_e((HF)_4) \approx 111$ to $119\,\mathrm{kJ\,mol^{-1}}$, fully consistent with the present theoretical result. The new results support our previous conjecture [56] that $(HF)_4$ should be stable with respect to dissociation upon HF stretching fundamental excitation, rendering a reinterpretation [56, 57] of recent predissociation-scattering experiments [58] quite likely.

### 4.2. *Barriers to concerted hydrogen exchange*

The computation of the barriers has proven to be significantly more difficult than the calculation of the dissociation energies. In fact, it is not possible to identify individual monomer fragments in the saddle point structures, and many-body decompositions and counterpoise corrections are not well defined. In any case, however, it is guaranteed that the procedure adopted in the present work will lead to the correct answers when the *ab initio* methods and basis sets are subsequently improved. Moreover, we are convinced that the calculations of the present work provide results that are as close to the true barriers as is achievable today from a computational point of view.

For the dimer and trimer, the computed barriers (178.0 and 87.4 kJ mol$^{-1}$, respectively) are 7–8 kJ mol$^{-1}$ higher than our previous estimates. This is a satisfactory agreement in view of the large error bars of 10 kJ mol$^{-1}$, which result from the very slow and counterpropagating convergence of this quantity with basis size and electronic structure level [4]. Thus, our best estimates for the barrier are coincidentally close to earlier DZP MP2 predictions [4, 16], while improvement of the basis set or the correlation treatment alone would lead to larger discrepancies. For the trimer, an unpublished full CCSD(T)/aug-cc-pVTZ saddle point optimization [52] confirms our structure assumption and yields a BSSE uncorrected barrier of 81.9 kJ mol$^{-1}$ (table 6).

More pronounced changes in the same direction are obtained for the tetramer and in particular for the pentamer. We find considerably larger barriers for these oligomers than anticipated in our earlier investigations. Note that there is a sizeable correlation contribution even for the four- and five-body terms. This contribution is not fully captured at MP2 level, but we can estimate the higher order effects from the DZP results. Thus, in the present study, we find that the tetramer may have a slightly lower barrier to concerted hydrogen exchange than the pentamer. There are only a few *ab initio* calculations available for comparison. Liedl *et al.* [19] and Maerker *et al.* [4] have performed MP2 and density functional calculations using a 6-311++ G(3df, 3pd) basis set, but the barriers computed with this basis set suffer from noticeable basis set limitations, as expected [4]. To illustrate the order of magnitude of the basis set effects, we include in table 6 our MP2 results obtained with the T/Q basis set, which is roughly comparable with the 6-311++G(3df, 3pd) basis set, even if it is slightly larger. For the dissociation energies, we observe counterpoise corrections of 6.0 kJ mol$^{-1}$ for the tetramer and 9.1 kJ mol$^{-1}$ for the pentamer. Due to the much shorter FF distances in the saddle point structures, we expect a larger BSSE for these structures than for the minimum energy structures. Indeed, the corresponding counterpoise corrections for the saddle points—assuming that they can be computed in the usual manner—are 15.8 and 20.5 kJ mol$^{-1}$, respectively. Thus, the barriers are increased by as much as 9.8 and 11.4 kJ mol$^{-1}$ by the counterpoise correction. At this point, of course, we do not consider changes in the geometries due to the BSSE, but without doubt, a correction of *ca.* 10 kJ mol$^{-1}$ is a reasonable estimate for the order of magnitude of the 6-311++G(3df, 3pd)-related BSSE at the MP2 level. Figures 2 and 3 provide a summary of various energies computed here, in a suitable graphical representation.

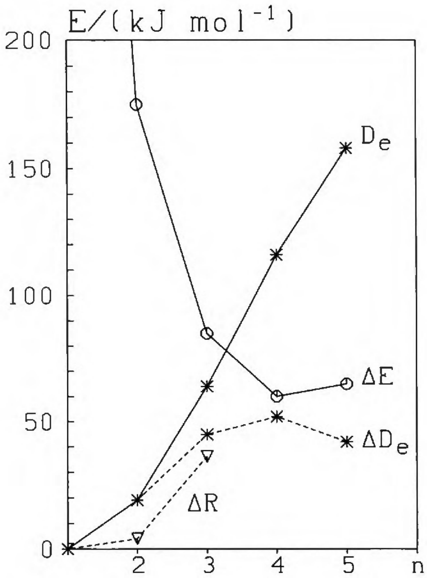

Figure 2. Dissociation energy ($D_e(n)$, stars, full line) for fragmentation of $(HF)_n$ into $n$ HF molecules, hydrogen bond dissociation energy of $(HF)_n$ into $(HF)_{n-1}$ and HF ($\Delta D_e(n) = D_e(n) - D_e(n-1)$, stars, dashed line), energy barrier ($\Delta E(n)$, circles, full line) for the concerted hydrogen exchange between binding sites (see equation (4)), and energy barrier ($\Delta R(n)$, triangles, dashed line) for hydrogen bond switching (see equation (2)), all as a function of cluster size $n$. Beyond $n = 3$, the simultaneous hydrogen exchange in the cluster becomes more facile than complete cluster dissociation into monomers, but dissociation of a *single* HF from the cluster requires less or comparable energy. Asymptotically, for large ring clusters, both $D_e(n)$ and $\Delta E(n)$ should become proportional to $n$, whereas $\Delta D_e(n)$ will approach a finite, constant value.

Despite the current uncertainty of the electronic barriers, an analysis of the unimolecular isomerization process in terms of simple transition state theory is useful [4]. In this framework, the thermal rate constant $k_{(3)}(T)$ corresponding to the process of equation (3) is

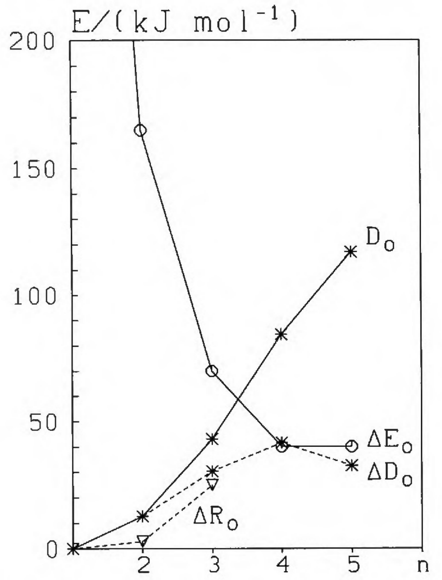

Figure 3. As figure 2, but now including zero point energy contributions to the dissociation energy into monomers ($D_0$), to the dissociation energy of a single monomer ($\Delta D_0$), to the barrier for hydrogen transfer ($\Delta E_0$, estimated harmonically) and to the barrier for hydrogen bond switching ($\Delta R_0$, estimated harmonically, see, however [59], where the harmonic approximation for this quantity was shown to be poor).

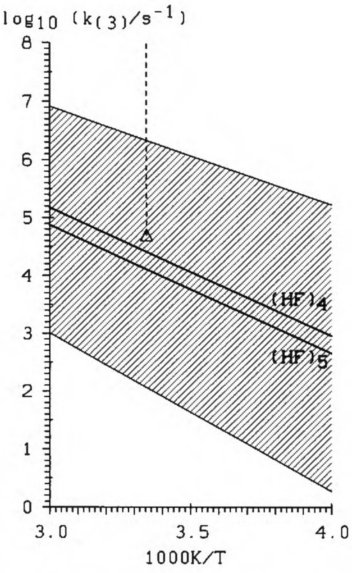

Figure 4. Decadic logarithm of the unimolecular hydrogen transfer rate $k_{(3)}$ in HF tetramers and pentamers from transition state theory without tunnelling (thick lines, the hatched region marks the theoretical uncertainty, which is dominated by the error bar for the barriers) as a function of reciprocal temperature $1/T$. For comparison, an experimental *lower* bound obtained in the gas phase at 299 K (independent of pressure) [21] is shown (triangle, the lower bound character is marked with dashes). Tunnelling will increase the rate by allowing transmission coefficients $\gamma_a > 0$ on each channel for energies $E \leqslant E_0$ (and $\leqslant$ channel maxima) but will also lead to a contribution decreasing the rate because of $\gamma_a < 1$ for $E \geqslant E_0$ (and $\geqslant$ channel maxima), say, in the framework of the adiabatic channel model [61]. Recent calculations by Loerting *et al.* [25 (b)] seem to indicate tunnelling corrections of about two orders of magnitude.

given by

$$k_{(3)}(T) = \frac{kT}{h}\frac{q^{\ddagger}_{\rm int}}{q_{\rm int}} \exp\left(-\Delta E_0/RT\right). \qquad (5)$$

The ratio of internal partition functions $q_{\rm int} = q_{\rm vib}q_{\rm rot}/\sigma$ between the $D_{nh}$ transition state (‡, symmetry number $\sigma^{\ddagger} = 2n$) and the $C_{nh}$ ground state (without superscript, $\sigma = n$) can be estimated in the harmonic approximation from *ab initio* calculations. For the experimentally relevant temperature range of 250–330 K, $q^{\ddagger}_{\rm int}/q_{\rm int}$ is found to be $0.04 \pm 0.02$ for the tetramer and $0.02 \pm 0.01$ for the pentamer, based on MP2 DZP [16], B3LYP and BHHLYP calculations [4]. A more significant uncertainty is inherent in the zero-point energy corrected transition state barriers, which we estimate to be $\Delta E_0 = 40 \pm 10\,{\rm kJ\,mol^{-1}}$ for both the tetramer and the pentamer of HF (figure 3). These estimates are based on the best available electronic barriers derived in this work together with harmonic zero-point energy contributions at MP2 DZP [16] and density functional levels [4], which agree within ±10%.

Very little is known experimentally about these concerted hydrogen exchange barriers in cyclic HF clusters. From the absence of a spin–spin coupling doublet in the vapour NMR spectra, Mackor *et al.* [21] concluded within the framework of simple transition state theory (neglecting differences in the partition functions for the $D_{nh}$ and $C_{nh}$ structures) that $\Delta E_0 < 48\,{\rm kJ\,mol^{-1}}$. Given the small ratio of $D_{nh}$ to $C_{nh}$ partition functions for $({\rm HF})_4$ and $({\rm HF})_5$ (*vide supra*), this upper bound is probably overestimated [4], although quantum tunnelling [25] may in part compensate for the partition function contribution even at room temperature [60] and anharmonic contributions represent a sizeable additional uncertainty [59]. Figure 4 compares experimental [21] and theoretical (equation (5)) results for the thermal rate constant $k_{(3)}(T)$. It is seen that the tetramer and the pentamer exhibit quite comparable exchange rates, which are close to the experimental lower bound of the gas phase rate at 299 K [21], namely $5 \times 10^4\,{\rm s^{-1}}$. Both larger [4] and smaller clusters will contribute much less to the exchange rate (see figure 3). Given the progress in NMR spectroscopy over the last three decades [62, 63], our results suggest that a reinvestigation of the vapour NMR spectra at lower temperatures (and pressures) might permit a detailed characterization of the spin coupling doublet coalescence. This would provide important experimental information on this prototypical hydrogen transfer process and on the subsequent cluster dissociation kinetics. As shown in figures 2 and 3, the latter two processes have similar activation energies for $(HF)_n$ (with $n = 4$ and 5). Hydrogen exchange in collisional complexes between HF oligomers ($2 < n < 5$) and HF molecules is thus already feasible at low collisional energies without quantum tunnelling contributions [25]. At very low vapour pressures, the collision process itself may become rate limiting, thus allowing for a study of the cluster association/dissociation kinetics. This might be feasible with modern high-field NMR spectrometers but is also within reach of current IR spectroscopic methods.

Two restrictions apply to our prediction of a microsecond or only slightly faster timescale for the loss of monomer integrity in clustered HF vapour at moderately low temperatures. (a) There could be sizeable quantum tunnelling [64] corrections to the transition state rate. A recent investigation [25] does not seem to support rate enhancements over many orders of magnitude for the temperatures and cluster sizes considered here, although large-curvature corrections seem to contribute about two orders of magnitude [25(b)]. The current uncertainty in the exchange barrier height ($\pm 10\,\mathrm{kJ\,mol^{-1}}$) may still dominate the overall uncertainty in the exchange rate, but in contrast to tunnelling contributions, it can increase or decrease the rate. Clearly, tunnelling is not efficient enough to lead to easily detectable splittings in the IR spectra [57], but a nanosecond exchange timescale would not be excluded by current experimental evidence. (b) There might be other tunnelling pathways with even lower barriers present in larger clusters, e.g. via ionic intermediates [49]. Strictly speaking, the existence of such competitive pathways cannot be rigorously excluded, although the enormous three-body enhancement (see table 4, part (b)) of the concerted process renders competitive non-concerted mechanisms rather unlikely. The fact that NMR spin-doublet coalescence can be suppressed in carefully neutralized *liquid* HF [21] would also tend to exclude such pathways.

In this context, one should note that hydrogen bond switching processes such as the well-characterized donor–acceptor hydrogen bond exchange (equation (2)) in the dimer [2, 59, 65] fully conserve monomer integrity. In figures 2 and 3, the barriers for these processes are given for the dimer and for the trimer [1], as obtained for the SO-3 potential energy hypersurface in combination with the HF3BG three-body potential. The barriers ($\Delta R$) lie below the lowest dissociation thresholds ($\Delta D$) for $(HF)_n$ with $n = 2$ and 3 but may in principle be larger for $n \geqslant 4$. However, one should note that *sequential* single monomer dissociation and association pathways for hydrogen bond switching are almost barrierless on the association side [16,18], in particular including zero-point energy. Therefore, a likely hydrogen bond switching scenario for larger ring clusters is the formation of the next smaller ring with a monomer loosely attached to it [18, 56, 66]. These attached monomers have a high peripheral mobility and can insert into the ring at another position, after which the next monomer can go to the periphery, etc. Such a *sequential* mechanism for hydrogen bond switching is unlikely to have a barrier $\Delta R$ significantly above the lowest dissociation threshold $\Delta D$. In contrast, *concerted* hydrogen bond rearrangements tend to be become disfavoured for larger rings due to the strengthening of the hydrogen bond. Finally, there is obviously more than one result of concerted rearrangements for $n > 3$, giving rise to different saddle points. These will be studied in more detail elsewhere together with several dozens of local cluster minima which we have characterized on the analytical potentials for $n = 4$–8 [16].

## 5. Conclusion

The potential hypersurfaces for hydrogen bonded systems govern some of the most important chemical processes, from inorganic vapour condensation and evaporation phenomena to biochemical DNA replication reactions and dynamics of enzymes. The cooperative nature of hydrogen bonding presents a substantial challenge to high level quantum chemistry approaches due to their unfavourable scaling with the number of atoms involved. Quantitative insights have been obtained here for the simple and well studied prototype system $(HF)_n$ through judicious decomposition into separately calculated many-body contributions. An important result is the rapid decline of $n$-body contributions with increasing $n$ *after* the three-body term, whereas two- and three-body terms are both essential for a description of the hydrogen bond in larger HF clusters. The detailed convergence pattern naturally depends on the investigated quantities, the geometries and the required accuracy. For a cluster of size $n > 3$, there will usually be special conformations for which even the highest (i.e. $n$-body) term is important, but in general these conformations will not be relevant for the hydrogen bond dynamics. Truncation after the three-body term is often found to be satisfactory for the hydrogen bond geometry and energetics, while hydrogen transfer barriers and some vibrational frequencies demand four-body contributions as well.

From $(HF)_2$ to $(HF)_5$, the electronic binding energy per hydrogen bond increases by 65%, the contribution of the pair potential to the hydrogen bond falls from 100 to about 60%, the three-body contribution rises from 0 to 40% and the concerted hydrogen exchange barrier per hydrogen drops to about 15% of its value in $(HF)_2$. Inclusion of zero-point energy further enhances some of the changes. The failure of density functional methods to describe the hydrogen exchange process turns out to be even more pronounced than expected. Further refinements on the cluster binding energies should include an explicit geometry optimization. The present results support previous IR spectroscopic analyses [56] and suggest that state of the art NMR gas phase studies should be able to quantitatively analyse the hydrogen exchange dynamics, whereas other types of kinetics studies would also be useful to investigate exchange processes in various mixed isotopomers $[(HF)_n(DF)_m]$, etc.

We would like to thank M. Borer, J. Brunson, C. Moor-Häberling, and U. Röthlisberger for the excellent and unbureaucratic support of our quantum chemical calculations, and T. Helgaker, K. R. Liedl, H. H. Limbach and H. F. Schaefer III for discussions and comments on the manuscript as well as the permission to cite from the unpublished work of [52]. We gratefully acknowledge generous allocations of computing resources by the Competence Centre of Computational Chemistry ($C^4$ project) in Zürich, the Centro Svizzero di Calcolo Scientifico (CSCS/SCSC) in Manno, Switzerland, and the computer centres of the University of Oslo and the University of Bergen. Our research is supported by the Schweizerischer Nationalfonds and by the Norwegian Research Council (Supercomputer Programme Grant No. NN2694K).

## References

[1] Quack, M., and Suhm, M. A., 1997, *Conceptual Perspectives in Quantum Chemistry, Conceptual Trends in Quantum Chemistry*, Vol. III, edited by J.-L. Calais and E. S. Kryachko (Dordrecht: Kluwer), pp. 415–463.

[2] Puttkamer, K. v., and Quack, M., 1989, *Chem. Phys.*, **139,** 31.

[3] Quack, M., and Suhm, M. A., 1991, *J. chem. Phys.*, **95,** 28.

[4] Maerker, C., von Ragué Schleyer, P., Liedl, K. R., Ha, T.-K., Quack, M., and Suhm, M. A., 1997, *J. comput. Chem.*, **18,** 1695. There is a misprint in the eighth line before the end of the Conclusions in this paper, where it should read 20 to 40 kJ mol$^{-1}$, of course.

[5] Klopper, W., Quack, M., and Suhm, M. A., 1996, *Chem. Phys. Lett.*, **261,** 35.

[6] Price, S. L., 1997, *Molecular Interactions—From van der Waals to Strongly Bound Complexes*, edited by S. Scheiner (New York: Wiley), Chap. 9, pp. 297–333.

[7] Rigby, M., Smith, E. B., Wakeham, W. A., and Maitland, G. C., 1986, *The Forces Between Molecules* (Oxford: Clarendon Press).

[8] Axilrod, B. M., and Teller, E., 1943, *J. chem. Phys.*, **11,** 299.

[9] DelBene, J. E., and Pople, J. A., 1971, *J. chem. Phys.*, **55,** 2296.

[10] Clark, J. H., Emsley, J., Jones, D. J., and Overill, R. E., 1981, *J. chem. Soc. Dalton Trans.*, 1219.

[11] Karpfen, A., Beyer, A., Schuster, P., 1983, *Chem. Phys. Lett.*, **102,** 289.

[12] Gaw, J. F., Yamaguchi, Y., Vincent, M. A., and Schaefer III, H. F., 1984, *J. Am. Chem. Soc.*, **106,** 3133.

[13] Liu, S., Michael, D. W., Dykstra, C. E., and Lisy, J. M., 1986, *J. chem. Phys.*, **84,** 5032.

[14] Latajka, Z., and Scheiner, S., 1988, *Chem. Phys.*, **122,** 413.

[15] Chałasiński, G., Cybulski, S. M., Szczęśniak, M. M., and Scheiner, S., 1989, *J. chem. Phys.*, **91,** 7048.

[16] Quack, M., Stohner, J., and Suhm, M. A., 1993, *J. molec. Struct.*, **294,** 33, and to be published.

[17] Chałasiński, G., and Szczęśniak, M. M., 1994, *Chem. Rev.*, **94,** 1723.

[18] Suhm, M. A., 1995, *Ber. Bunsenges. Phys. Chem.*, **99,** 1159.

[19] Liedl, K. R., Kroemer, R. T., and Rode, B. M., 1995, *Chem. Phys. Lett.*, **246,** 455.

[20] Hindermann, D. K., and Cornwell, C. D., 1968, *J. chem. Phys.*, **48,** 2017.

[21] Mackor, E. L., MacLean, C., and Hilbers, C. W., 1968, *Recl. Trav. Chim.*, **87,** 655.

[22] Heidrich, D., Köhler, H. J., and Volkmann, D., 1985, *Int. J. quant. Chem.*, **27,** 781.

[23] Karpfen, A., 1990, *Int. J. quantum Chem.* (*Quant. Chem. Symp.*), **24,** 129.

[24] Komornicki, A., Dixon, D. A., and Taylor, P. R., 1992, *J. chem. Phys.*, **96,** 2920.

[25] (a) Liedl, K. R., Sekušak, S., Kroemer, R. T., and Rode, B. M., 1997, *J. phys. Chem.* A, **101,** 4707; (b) Loerting, T., Liedl, K. R., and Rode, B. M., 1998, *J. Am. Chem. Soc.* (in the press).

[26] Pedulla, J. M., Vila, F., and Jordan, K. D., 1996, *J. chem. Phys.*, **105,** 11091.

[27] Tschumper, G. S., Yamaguchi, Y., and Schaefer III, H. F., 1997, *J. chem. Phys.*, **106,** 9627.

[28] v. Duijneveldt, F. B., 1997, *Molecular Interactions—From van der Waals to Strongly Bound Complexes*, edited by S. Scheiner (New York: Wiley), Chap. 3, pp. 81–104.

[29] Tachikawa, M., and Iguchi, K., 1994, *J. chem. Phys.*, **101,** 3062.

[30] Xantheas, S. S., 1994, *J. chem. Phys.*, **100,** 7523.

[31] Noga, J., Kutzelnigg, W., and Klopper, W., 1992, *Chem. Phys. Lett.*, **199,** 497.

[32] Noga, J,, and Kutzelnigg, W., 1994, *J. chem. Phys.*, **101,** 7738.

[33] Noga, J., Klopper, W., and Kutzelnigg, W., 1997, *Recent Advances in Coupled-Cluster Theory*, Recent Advances in Computational Chemistry, Vol. III, edited by R. J. Bartlett (Singapore: World Scientific Publishers), pp. 1–48.

[34] Klopper, W., and Noga, J., 1995, *J. chem. Phys.*, **103,** 6127.

[35] Müller, H., Kutzelnigg, W., Noga, J., and Klopper, W., 1997, *J. chem. Phys.*, **106,** 1863.

[36] Helgaker, T., Klopper, W., Koch, H., and Noga, J., 1997, *J. chem. Phys.*, **106,** 9639.

[37] Klopper, W., 1991, `SORE` program.

[38] Noga, J., and Klopper, W., 1995, `DIRCCR12` program.

[39] Frisch, M. J., Trucks, G. W., Schlegel, H. B., Gill, P. M. W., Johnson, B. G., Robb, M. A., Cheeseman, J. R., Keith, T., Petersson, G. A., Montgomery, J. A., Raghavachari, K., Al-Laham, M. A., Zakrzewski, V. G., Ortiz, J. V., Foresman, J. B., Cioslowski, J., Stefanov, B. B., Nanayakkara, A., Challacombe, M., Peng, C. Y., Ayala, P. Y., Chen, W., Wong, M. W., Andres, J. L., Replogle, E. S., Gomperts, R., Martin, R. L., Fox, D. J., Binkley, J. S., Defrees, D. J., Baker, J., Stewart, J. P., Head-Gordon, M., Gonzales, C., and Pople. J. A., 1995, `Gaussian94, Revisions C.3 and D.2` (Pittsburgh, PA: Gaussian Inc).

[40] Klopper, W., Quack, M., and Suhm, M. A., 1998, *J. chem. Phys.* (submitted).

[41] Dunning Jr, T. H., 1989, *J. chem. Phys.*, **90,** 1007.

[42] Kendall, R. A., Dunning Jr, T. H., and Harrison, R. J., 1992, *J. chem. Phys.*, **96,** 6796.

[43] Dunning Jr, T. H., unpublished.

[44] The aug-cc-pVXZ basis sets (X = T, Q, 5) were obtained from the Extensible Computational Chemistry Environment Basis Set Database, Version 1.0, as developed and distributed by the Molecular Science Computing Facility, Environmental and Molecular Sciences Laboratory which is part of the Pacific Northwest Laboratory, PO Box 999, Richland, Washington 99352, USA, and funded by the US Department of Energy. The Pacific Northwest Laboratory is a multi-program laboratory operated by Battelle Memorial Institute for the US Department of Energy under contract DE-AC06-76RLO 1830. Contact David Feller, Karen Schuchardt, or Don Jones for further information.

[45] Mayer, I., and Surjan, P. R., 1992, *Chem. Phys. Lett.*, **191,** 497.

[46] Xantheas, S. S., 1996, *J. chem. Phys.*, **104,** 8821.

[47] Chang, Y.-T., and Miller, W. H., 1990, *J. chem. Phys.*, **94,** 5884.

[48] Quack, M., and Suhm, M. A., 1996, *Theor. Chim. Acta*, **93,** 61.

[49] Heidrich, D., van Eikema Hommes, N. J. R., and von Ragué Schleyer, P., 1993, *J. Comput. Chem.*, **14,** 1149.

[50] Collins, C. L., Morihashi, K., Yamaguchi, Y., and Schaefer III, H. F., 1995, *J. chem. Phys.*, **103,** 6051.

[51] Peterson, K. A., and Dunning Jr, T. H., 1995, *J. chem. Phys.*, **102,** 2032.

[52] Liedl, K. R., Xantheas, S. S., Rode, B. M., and Dunning, Jr., T. H. J., 1997, private communication.

[53] Novoa, J. J., Planas, M., and Whangbo, M.-H., 1994, *Chem. Phys. Lett.*, **225,** 240.

[54] Suhm, M. A., and Nesbitt, D. J.,1995, *Chem. Soc. Rev.*, **24,** 45.

[55] Miller, R. E., 1990, *Acc. Chem. Res.*, **23,** 10.

[56] Luckhaus, D., Quack, M., Schmitt, U., and Suhm, M. A., 1995, *Ber. Bunsenges. Phys. Chem.*, **99,** 457.

[57] Quack, M., Schmitt, U., and Suhm, M. A., 1997, *Chem. Phys. Lett.*, **269,** 29.

[58] Huisken, F., Kaloudis, M., Kulcke, A., Laush, C., and Lisy, J. M., 1995, *J. chem. Phys.*, **103,** 5366.

[59] Quack, M., and Suhm, M. A., 1991, *Chem. Phys. Lett.*, **183,** 187.

[60] Stöckli, A., Meier, B. H., Kreis, R., Meyer, R., and Ernst, R. R., 1990, *J. chem. Phys.*, **93,** 1502.

[61] Quack, M., and Troe, J., 1998, *Encyclopedia of Computational Chemistry* (New York: Wiley) (in the press). See also Quack, M., and Troe, J., 1981, *Theor. Chem. Adv. Pesp.*, **6B,** 199.

[62] Limbach, H. H., Scherer, G., Meschede, L., Aguilar-Parrilla, F., Wehrle, B., Braun, J., Hoelger, C., Benedict, H., Buntkowsky, G., Fehlhammer, W. P., Elguero, J., Smith, J. A. S., and Chaudret, B.,1994, *AIP Conference Proceedings (298): Ultrafast Reaction Dynamics and Solvent Effects* , Part III, edited by Y. Gauduel and P. J. Rossky (American Institute of Physics), pp. 225–239.

[63] Ernst, R. R., Bodenhausen, G., and Wokaun, A., 1987, 1994, *Principles of Nuclear Magnetic Resonance in One and Two Dimensions* (Oxford: Clarendon Press).

[64] Drukker, K., and Hammes-Schiffer, S., 1997, *J. chem. Phys.*, **107,** 363.

[65] Dyke, T. R., Howard, B. J., and Klemperer, W., 1972, *J. chem. Phys.*, **56,** 2442.

[66] Huisken, F., Tarakanova, E. G., Vigasin, A. A., and Yukhnevich, G. V., 1995, *Chem. Phys. Lett.*, **245,** 319.